scientific reports

Check for updates

OPEN

Rapid in vitro quantification of TDP-43 and FUS mislocalisation for screening of gene variants implicated in frontotemporal dementia and amyotrophic lateral sclerosis

Lisa J. Oyston[1], Stephanie Ubiparipovic[1,2], Lauren Fitzpatrick[1], Marianne Hallupp[1], Lauren M. Boccanfuso[1], John B. Kwok[1] & Carol Dobson-Stone[1]✉

Identified genetic mutations cause 20% of frontotemporal dementia (FTD) and 5-10% of amyotrophic lateral sclerosis (ALS) cases: however, for the remainder of patients the origin of disease is uncertain. The overlap in genetic, clinical and pathological presentation of FTD and ALS suggests these two diseases are related. Post-mortem, ~95% of ALS and ~50% of FTD patients show redistribution of the nuclear protein TDP-43 to the cytoplasm within affected neurons, while ~5% ALS and ~10% FTD show mislocalisation of FUS protein. We exploited these neuropathological features to develop an unbiased method for the in vitro quantification of cytoplasmic TDP-43 and FUS. Utilising fluorescently-tagged cDNA constructs and immunocytochemistry, the fluorescence intensity of TDP-43 or FUS was measured in the nucleus and cytoplasm of cells, using the freely available software CellProfiler. Significant increases in the amount of cytoplasmic TDP-43 and FUS were detectable in cells expressing known FTD/ALS-causative *TARDBP* and *FUS* gene mutations. Pharmacological intervention with the apoptosis inducer staurosporine and mutation in a secondary gene (*CYLD*) also induced measurable cytoplasmic mislocalisation of endogenous FUS and TDP-43, respectively. These findings validate this methodology as a novel in vitro technique for the quantification of TDP-43 or FUS mislocalisation that can be used for initial prioritisation of predicted FTD/ALS-causative mutations.

Frontotemporal dementia (FTD) is one of the most common forms of presenile dementia and involves the progressive degeneration of the frontal and temporal lobes of the brain. Amyotrophic lateral sclerosis (ALS) is a progressive neurodegenerative disorder that affects the upper and lower motor neurons leading to muscle weakness and paralysis[1]. Increasing genetic evidence, neuropathological and clinical observations have identified a substantial overlap between these two disorders[2]. Several genes have been identified where mutations can cause either FTD or ALS (FTD-ALS genes) including *C9orf72*, *VCP*, *OPTN*, *SQSTM1*, *TBK1*[3] and, most recently, *CYLD*[4]. In addition, FTD and ALS share neuropathological similarities: ~95% of ALS and ~50% of FTD patients show cytoplasmic inclusions of TAR DNA-binding protein 43 (TDP-43) in the brain[5,6], while ~5% of ALS and ~10% of FTD patients show cytoplasmic inclusions of fused in sarcoma protein (FUS)[6–8]. In healthy cells, TDP-43 and FUS are largely expressed within the nucleus. In FTD and ALS, affected neurons can display a redistribution of TDP-43 or FUS to the cytoplasm, as well as insoluble TDP-43 or FUS aggregates[6,9,10]. The importance of TDP-43 and FUS is further demonstrated by the fact that mutation of their encoding genes *TARDBP* and *FUS* is sufficient to cause ALS[7,11,12] or, rarely, FTD[13].

Identified genetic mutations cause 20% of FTD and 5-10% of ALS cases[14,15]; however, for the remainder of patients the origin of the disease is uncertain. Despite TDP-43 being a prominent feature in the majority of FTD and ALS cases, including all those carrying FTD-ALS gene mutations[13], this fact has not been applied to the

[1]Brain and Mind Centre and School of Medical Sciences, Faculty of Medicine and Health, The University of Sydney, Camperdown, NSW 2006, Australia. [2]Garvan Institute of Medical Research, Darlinghurst, NSW 2010, Australia. ✉email: carol.dobson-stone@sydney.edu.au

screening of FTD and ALS candidate gene variants on a large scale. In previous studies, TDP-43 and FUS mislocalisation has largely been assessed by subcellular fractionation, immunohistochemistry and manual analysis of confocal microscopy[7,16–24] or high-content imaging[25–27]. Whilst studies utilising these techniques have been informative, these assays are labour intensive and low-throughput or, expensive and in some cases produce qualitative data. In addition, some microscopy-based techniques could be subject to bias due to manual selection of the cells to be analysed.

Here we report the development of a rapid, cheap and unbiased technique for the in vitro study of TDP-43 and FUS cytoplasmic mislocalisation. TDP-43 or FUS staining in nuclear and cytoplasmic subcellular compartments was measured in thousands of cells from confocal microscope images, using the freely available analysis software CellProfiler[28]. We validated this technique using known genetic drivers of TDP-43 or FUS mislocalisation. We were able to detect increased cytoplasmic localisation of exogenously expressed *FUS* and *TARDBP* mutations relative to wild-type (WT) sequence. We also observed mislocalisation of endogenous FUS upon treatment with the apoptosis inducer staurosporine. Importantly, we could also detect more subtle changes in the cellular distribution of endogenous TDP-43, arising from mutation in a secondary gene (*CYLD* p.M719V). This validated methodology can now be utilised for rapidly prioritising newly discovered FTD and ALS gene variants by quantifying their effect on TDP-43 and/or FUS localisation.

Results

Detection of FUS cytoplasmic mislocalisation with exogenous expression of FUS mutations. In order to validate our method for the unbiased quantification of FUS and TDP-43 mislocalisation we initially utilised known pathogenic *FUS* mutations that drastically alter FUS subcellular localisation[7,29]. Expression of green fluorescent protein (GFP)-tagged FUS protein with missense mutation FUS_{R521C} or truncation mutant FUS_{R495X} in the neuronal-like neuroblastoma cell line, SH-SY5Y, led to a significant increase in the fluorescence intensity of cytoplasmic FUS (Fig. 1e–k) when compared to FUS_{WT} (Fig. 1a–c,h). This increase in cytoplasmic FUS was accompanied by a corresponding decrease in the fluorescence intensity of nuclear FUS (Fig. 1d). Together, these resulted in a 9.5- and 12.5-fold increase in the FUS cytoplasmic/nuclear ratio for cells expressing FUS_{R521C} (0.97 ± 0.04; $p < 0.0001$) and FUS_{R495X} (1.28 ± 0.04; $p < 0.0001$), respectively, relative to FUS_{WT} (0.10 ± 0.00; Fig. 1l). Similar results were found when overexpressing the FUS_{R521C} (1.04 ± 0.05; $p < 0.0001$) and FUS_{R495X} (1.81 ± 0.10; $p < 0.0001$) mutants in human embryonic kidney (HEK293) cells (Supplementary Fig. S1), although the decrease in nuclear fluorescence intensity of FUS was not as prominent (Supplementary Fig. S1).

Detection of endogenous FUS cytoplasmic mislocalisation following staurosporine treatment. To test our ability to quantify the subcellular distribution of endogenous FUS we utilised the apoptosis inducer staurosporine, which has been previously reported to cause cytoplasmic mislocalisation of FUS[16]. Application of increasing doses of staurosporine showed an increase in the fluorescence intensity of cytoplasmic FUS in cells treated with the two highest doses of staurosporine (1 and 10 μM; Fig. 2a–d,f). A corresponding decrease in the nuclear intensity of FUS was also seen in SH-SY5Y cells (Fig. 2e). There was a significant increase of cytoplasmic/nuclear FUS ratio for all treatment groups (0.1 μM: 0.13 ± 0.01; $p = 0.0405$; 1 μM: 0.33 ± 0.05; $p = 0.0152$; 10 μM: 1.53 ± 0.12; $p = 0.0002$) relative to vehicle-treated cells (0.09 ± 0.00; Fig. 2g). HEK293 cells treated with staurosporine also exhibited a dose–response effect on FUS subcellular localisation. In general, HEK293 cells were more tolerant of the staurosporine treatment (Supplementary Fig. S2) as shown by the lower cytoplasmic/nuclear ratios observed when compared to the SH-SY5Y cells (Fig. 2g and Supplementary Fig. S2). Treatment with 10 μM staurosporine caused the majority of FUS to be present in the cytoplasm rather than the nucleus in SH-SY5Y cells (1.53 ± 0.12; $p = 0.0002$; Fig. 2d,g) whilst the same treatment in the HEK293 cells caused only a small proportion of FUS protein to be mislocalised (0.28 ± 0.01; $p < 0.0001$; Supplementary Fig. S2). Despite these differences in effect size, we could detect a significant effect of staurosporine treatment on mislocalisation of endogenous FUS in both cell lines.

Detection of TDP-43 cytoplasmic mislocalisation with exogenous expression of *TARDBP* mutations. We took the same initial approach used for FUS to validate this method for the quantification of TDP-43 cytoplasmic mislocalisation: i.e. exogenous expression of known pathogenic mutations in *TARDBP*. We examined p.A315T, one of the earliest detected and thus most extensively examined mutations[30–32], and two of the mutations most commonly observed in ALS patients: p.M337V and p.A382T[11,31–33].

In SH-SY5Y cells, a significant increase in the cytoplasmic/nuclear ratio of GFP-tagged $TDP\text{-}43_{A315T}$ (0.87 ± 0.01; $p = 0.0016$; Fig. 3b,f,i–k) and $TDP\text{-}43_{A382T}$ (0.86 ± 0.02; $p = 0.0032$; Fig. 3d,h–k) was observed when compared to $TDP\text{-}43_{WT}$ (0.75 ± 0.01; Fig. 3a,e,i–k). In contrast, there was a significant decrease in the cytoplasmic/nuclear ratio of GFP-tagged $TDP\text{-}43_{M337V}$ (0.63 ± 0.01; $p = 0.0028$; Fig. 3c,g,i–k) relative to $TDP\text{-}43_{WT}$. Similar to the experiments with FUS, expression of TDP-43 mutations had a lesser effect in HEK293 cells (Supplementary Fig. S3). Once again, there was a significant increase in the cytoplasmic/nuclear ratio of $TDP\text{-}43_{A315T}$ (0.57 ± 0.02; $p = 0.0021$; Supplementary Fig. S3) and $TDP\text{-}43_{A382T}$ cells (0.66 ± 0.03; $p = 0.0026$; Supplementary Fig. S3) when compared to $TDP\text{-}43_{WT}$ (0.50 ± 0.02; Supplementary Fig. S3). However, no significant effect was observed in $TDP\text{-}43_{M337V}$ cells (0.52 ± 0.01; Supplementary Fig. S3).

Detection of endogenous TDP-43 cytoplasmic mislocalisation in cells expressing a causative FTD/ALS mutation. To demonstrate the potential of this methodology for identifying potentially pathogenic variants in other FTD/ALS genes, we expressed a known familial FTD/ALS-causative mutation in the *CYLD* gene, p.M719V[4], and observed the changes in endogenous TDP-43 localisation. We previously determined that overexpression of $CYLD_{M719V}$ increases the proportion of cytoplasmic TDP-43-positive mouse primary cor-

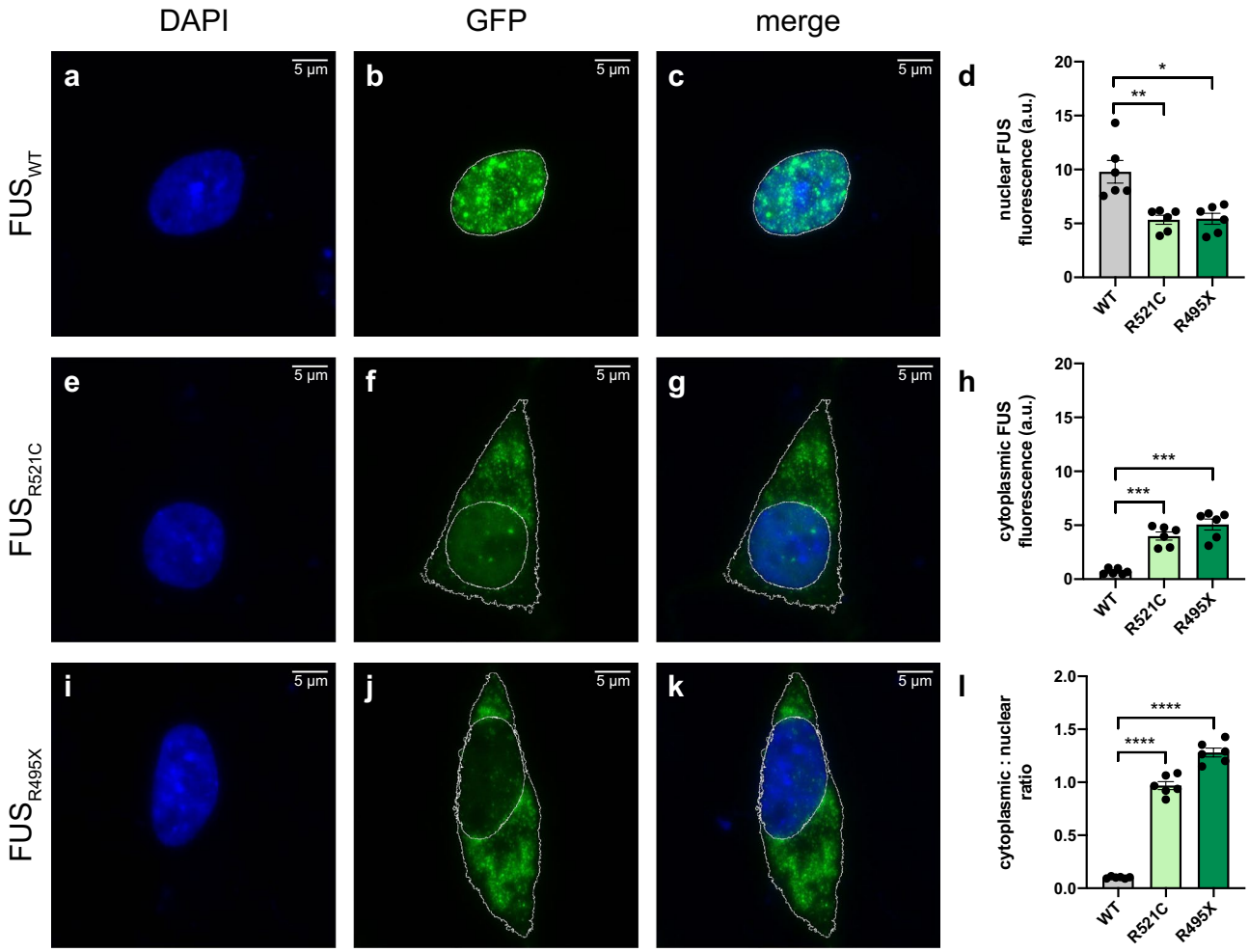

Figure 1. Detection of FUS cytoplasmic mislocalisation with exogenous expression of *FUS* mutations. Representative images of SH-SY5Y cells overexpressing GFP-tagged (**a**–**c**) FUS_{WT}, (**e**–**g**) FUS_{R521C} or (**i**–**k**) FUS_{R495X}. Nuclei were visualised with DAPI (blue). (**d**) Quantification of the fluorescence intensity of the nucleus shows a significant reduction in nuclear FUS expression in cells expressing FUS_{R521C} or FUS_{R495X}, when compared to FUS_{WT}. (**h**) Quantification of the fluorescence intensity of cytoplasmic FUS shows significantly higher cytoplasmic FUS expression in FUS_{R521C} and FUS_{R495X}, when compared to FUS_{WT}. (**l**) Quantification of the cytoplasmic/nuclear ratio of exogenous FUS shows a marked increase in FUS_{R521C}- and FUS_{R495X}-expressing cells when compared to FUS_{WT}. Scale bars = 5 µm. Data is represented as mean ± SEM. a.u. = arbitary units. *p < 0.05; **p < 0.01; ***p < 0.001; ****p < 0.0001.

tical neurons by ~ 20% when compared to $CYLD_{WT}$[4]. When compared to GFP-only vector control (0.079 ± 0.001; Fig. 4a–d), expression of $CYLD_{WT}$-GFP (Fig. 4e–h) in SH-SY5Y cells led to a significant 1.2-fold increase in the TDP-43 cytoplasmic/nuclear ratio (0.095 ± 0.001; p = 0.0002; Fig. 4q–s). In turn, expression of $CYLD_{M719V}$-GFP (Fig. 4m–p) caused a further 1.3-fold increase in cytoplasmic/nuclear TDP-43 relative to $CYLD_{WT}$-GFP (0.121 ± 0.002; p < 0.0001; Fig. 4q–s). The $CYLD_{M719V}$ mutation had the same effect in HEK293 cells, causing a 1.3-fold increase in the cytoplasmic/nuclear ratio relative to $CYLD_{WT}$ (0.145 ± 0.007; p = 0.0115; Supplementary Fig. S4). We also transfected cells with the $CYLD_{D681G}$ mutation (Fig. 4i–l and Supplementary Fig. S4) which is catalytically inactive and known to cause CYLD cutaneous syndrome, a skin tumour disorder[34,35]. Our data corroborated previous results[4] that the $CYLD_{D681G}$ mutation had no effect on TDP-43 localisation when compared to the GFP-only vector control in either cell type (Fig. 4s and Supplementary Fig. S4).

Discussion

In this study we have validated a novel methodology for the unbiased quantification of cytoplasmic TDP-43 and FUS in human cell lines under three different experimental paradigms: determining localisation of exogenously expressed mutant TDP-43 or FUS; detecting the effect of a chemical modulator on endogenous FUS localisation; and detecting the effect of a secondary gene on endogenous TDP-43 localisation. This rapid, cheap, quantitative assay can now be utilised for rapidly assessing drug treatments and the potential pathogenicity of newly discovered FTD and ALS gene variants by quantifying their effect on TDP-43 and/or FUS localisation.

Previous studies examining TDP-43 and FUS have quantified cytoplasmic mislocalisation in different ways. Many studies have reported the proportion of the cell population that display cytoplasmic TDP-43 or FUS

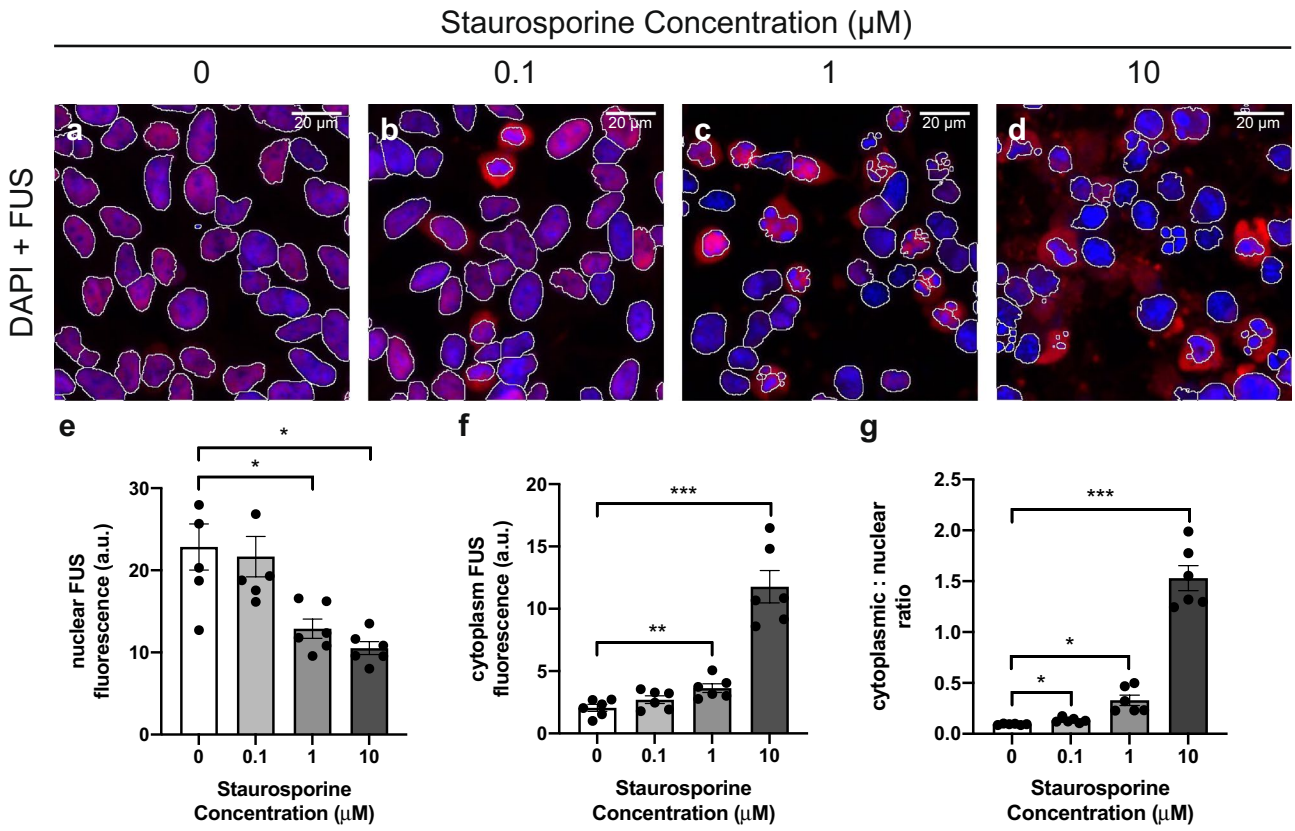

Figure 2. Detection of endogenous FUS cytoplasmic mislocalisation following staurosporine treatment. (**a**–**d**) Representative fluorescence images of SH-SY5Y cells treated with increasing concentrations of staurosporine. FUS was detected by immunofluorescent staining (red) and nuclei were visualised with DAPI (blue). (**e**) Quantification of nuclear and (**f**) cytoplasmic FUS fluorescence intensity show significant changes in 1 μM- and 10 μM-treated cells. (**g**) Quantification of the FUS cytoplasmic/nuclear ratio shows an increase in all treatment groups when compared to those treated with DMSO alone. Scale bars = 20 μm. Data is represented as mean ± SEM. *a.u.* arbitrary units. *p < 0.05; **p < 0.01; ***p < 0.001.

expression[12,18,19,21,24]. This may present a problem with reproducibility, since fluorescence detection thresholds for considering a cell as 'positive' for cytoplasmic protein likely differ between labs and will vary according to the microscopy equipment used. We selected the ratio of cytoplasmic to nuclear expression as our primary measure, having observed reduced variability between experimental replicates in comparison to individual nuclear and cytoplasmic measurements. Some studies have reported similar measurements using techniques such as high-content screening confocal microscopy to study TDP-43 or FUS mislocalisation under different conditions[25,26]. Whilst high-content screening can allow for a more high-throughput study design than our methodology, the extensive infrastructure required is expensive, not readily available and can require substantial optimisation. We note that while we selected the CellProfiler program for post-imaging analysis, other software platforms are capable of the same type of analysis e.g. Imaris (RRID:SCR_007370), ImageJ[36] and Huygens (RRID:SCR_014237). We chose CellProfiler based on its ease of use, the ability to perform batch analysis of images, cost and accessibility.

Another general observation in our experiments was that SH-SY5Y cells often displayed a greater degree of cytoplasmic mislocalisation than that in HEK293 cells under the same conditions. This may be due to SH-SY5Y cells being a neuronal cell line and thus more disease relevant, or due to the longer transfection time required to achieve optimal transfection efficiency in SH-SY5Y cells (48 h, versus 24 h in HEK293), causing additional stress on the cells. It should also be noted that transfection efficiency also dictated the number of images required to reach the desired cell number per replicate (300 cells). SH-SY5Y cells, which had a lower transfection efficiency, required more images to achieve the same number of cells for quantification.

The cytoplasmic mislocalisation and/or aggregation of FUS in neurons and glia of post-mortem tissue from patients with ALS caused by *FUS* mutations has been widely established[7,12]. This pathology has been recapitulated by expression of FUS mutations in mammalian cells[7,12,29]. In this study, exogenous expression of the severe truncation mutation FUS_{R495X} caused the majority of FUS to be mislocalised to the cytoplasm as previously demonstrated by Bosco et al.[29] using live-cell confocal microscopy and 3D images (11–28 cells). Our quick and simple methodology was able to duplicate these results using 2D images and a larger number of cells (1800 cells total). While we recognise the merits of quantifying the entire cell volume, measuring such a small number of selected cells is not representative of the population and may not be able to detect more subtle or variable effects in protein localisation.

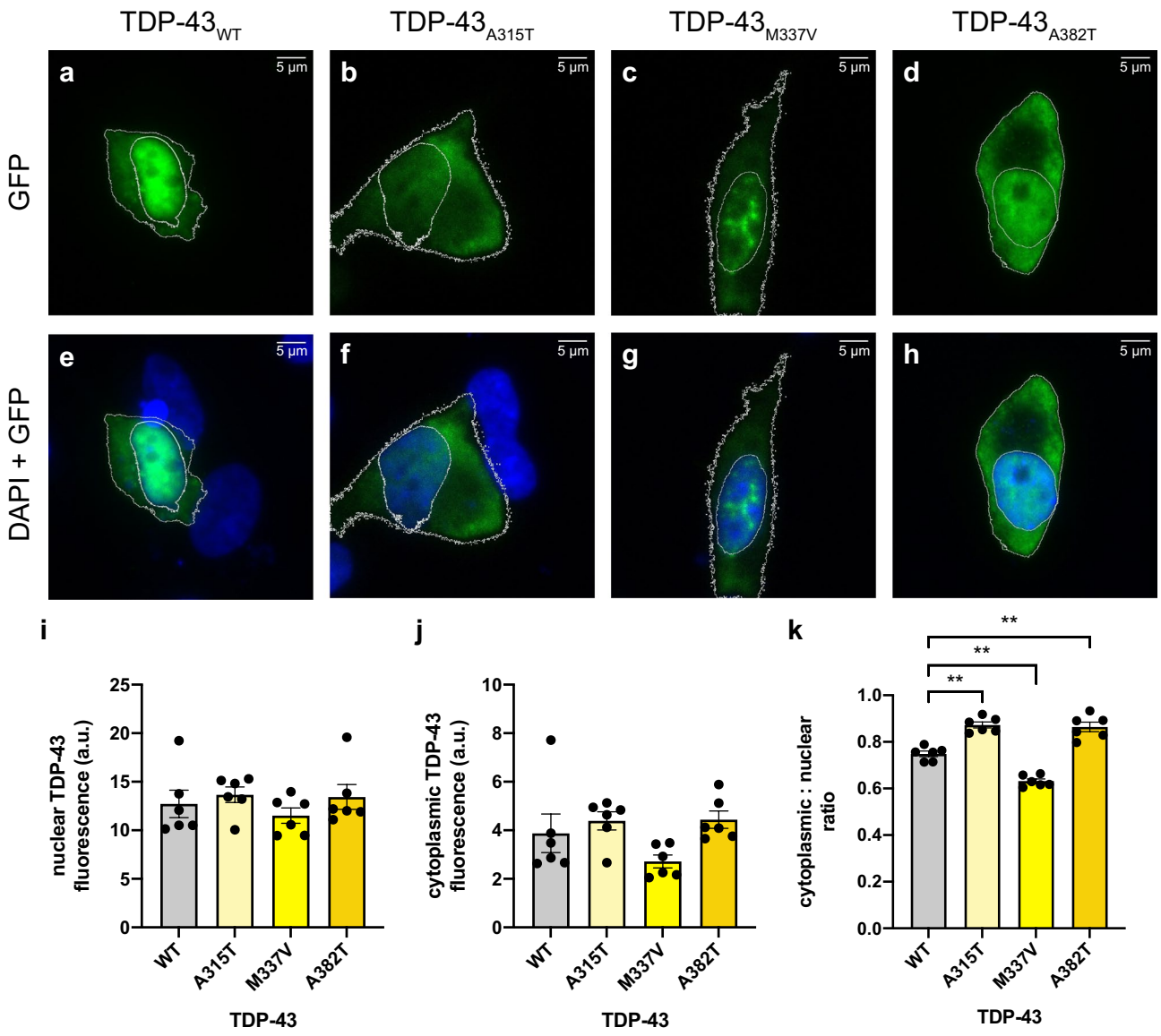

Figure 3. Detection of TDP-43 cytoplasmic mislocalisation with exogenous expression of *TARDBP* mutations. Representative images of SH-SY5Y cells overexpressing GFP-tagged (**a**,**e**) TDP-43_{WT}, (**b**,**f**) TDP-43_{A315T}, (**c**,**g**) TDP-43_{M337V} or (**d**,**h**) TDP-43_{A382T}. Nuclei were visualised with DAPI (blue). (**i**) Quantification of the fluorescence intensity of the nucleus and (**j**) the cytoplasm shows no significant difference in TDP-43 expression. (**k**) Quantification of the cytoplasmic/nuclear ratio of exogenous TDP-43 shows a significant increase in TDP-43_{A315T} and TDP-43_{A382T}, and a decrease in TDP-43_{M337V}, when compared to cells expressing TDP-43_{WT}. Scale bars = 5 µm. Data is represented as mean ± SEM. *a.u.* arbitrary units. $^{**}p < 0.01$.

Expression of the FUS_{R521C} missense mutation and treatment with staurosporine (1–10 µM) also reproduced previous qualitative microscopy and subcellular fractionation results[7,16,37] showing a significant increase in the FUS cytoplasmic/nuclear ratio. Confirmation of these results demonstrates the effectiveness of this new methodology in providing quantitative data where previously qualitative or labour-intensive experiments were required. Our ability to quantify FUS cytoplasmic mislocalisation following staurosporine treatment also demonstrates the possibility of this technique for use in testing the ability of novel FTD and ALS drug treatments to modulate FUS or TDP-43 mislocalisation.

The majority (~95%) of ALS and ~50% of FTD cases are characterised by the abnormal accumulation of TDP-43 in the cytoplasm of neurons and glia, even though in most cases mutations in *TARDBP* are absent[6]. Mutations in *TARDBP* have been associated with both FTD and ALS and lead to TDP-43 cytoplasmic mislocalisation[11,13]. Unlike FUS, the expression of *TARDBP* mutations in primary cells and cell lines does not reproduce the dramatic cytoplasmic mislocalisation seen in post-mortem tissue[38–40]. In addition, overexpression of exogenous TDP-43 in vitro is sufficient to induce mislocalisation even for WT sequence[19,23]. Any differences between WT and mutant TDP-43 for this characteristic are therefore harder to discern and represent a significant limitation for all TDP-43 exogenous expression assays, including the one described here, and may be responsible for differing results being reported for the same mutations. Our technique was able to detect a significant increase in

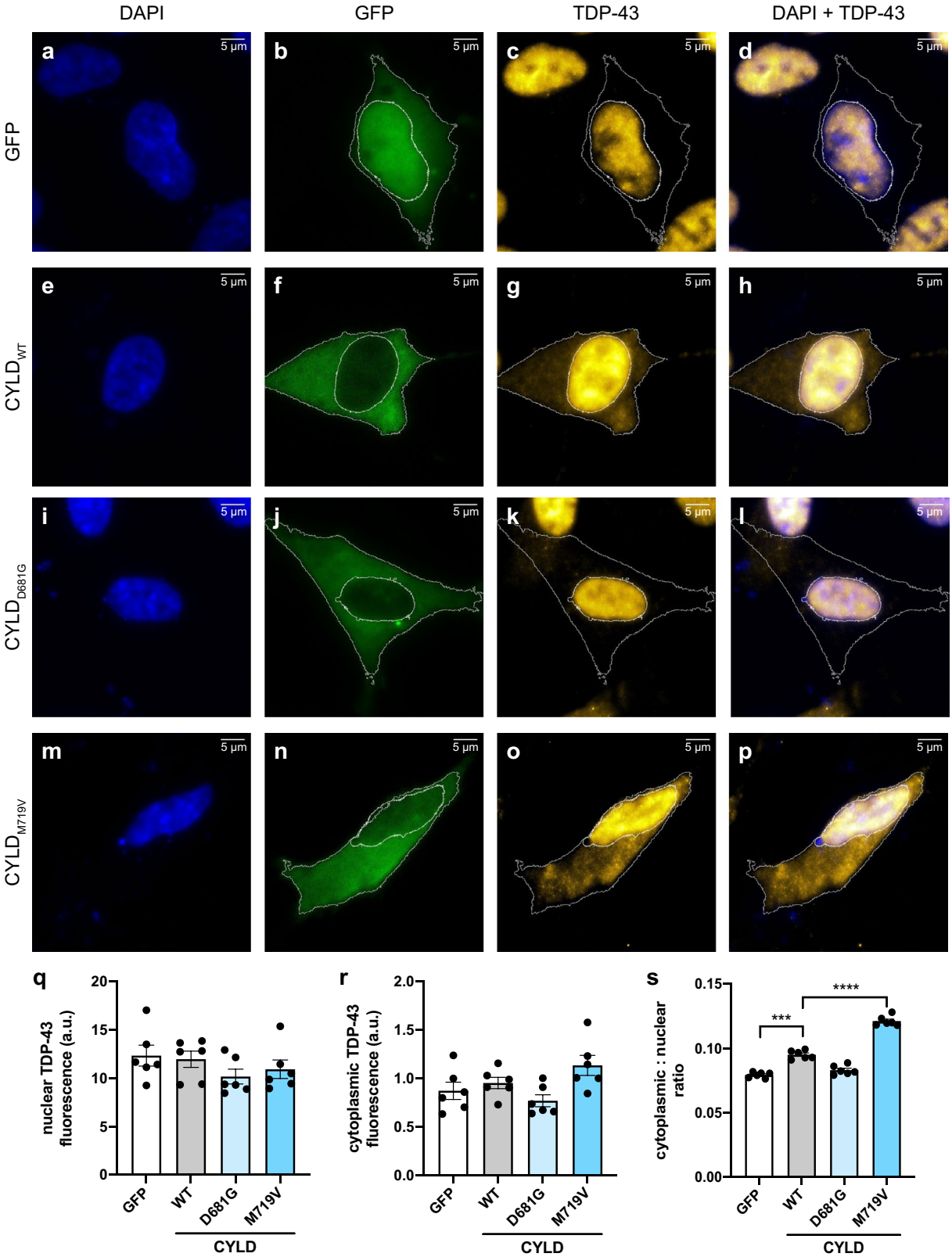

Figure 4. Detection of endogenous TDP-43 cytoplasmic mislocalisation in cells expressing *CYLD* mutations. Representative images of SH-SY5Y cells overexpressing (**a**–**d**) GFP or GFP-tagged (**e**–**h**) $CYLD_{WT}$, (**i**–**l**) $CYLD_{D681G}$ or (**m**–**p**) $CYLD_{M719V}$. TDP-43 was detected by immunofluorescent staining (yellow) and nuclei were visualised with DAPI (blue). (**q**) Quantification of the fluorescence intensity of the nucleus and (**r**) cytoplasm shows no difference in TDP-43 expression. (**s**) Quantification of the cytoplasmic/nuclear ratio of exogenous TDP-43 shows a marked increase in $CYLD_{WT}$, when compared to cells expressing GFP. The cytoplasmic/nuclear ratio of TDP-43 in $CYLD_{M719V}$-expressing cells was significantly higher than $CYLD_{WT}$. Scale bars = 5 µm. Data is represented as mean ± SEM. *a.u.* arbitrary units. ***$p < 0.001$; ****$p < 0.0001$.

the TDP-43 cytoplasmic/nuclear ratio in TDP-43_{A315T} and TDP-43_{A382T} cells when compared to TDP-43_{WT}. This confirms previous results for TDP-43_{A315T}[18,19] and TDP-43_{A382T}[41,42]. The TDP-43_{M337V} variant, which displayed a significant decrease in cytoplasmic TDP-43 in SH-SY5Y cells, has previously been shown to increase cytoplasmic TDP-43 in some[19,21,24], but not all studies[22]. We note that TDP-43_{M337V} has previously been shown to aggregate into nuclear puncta in SH-SY5Y cells[21], which we observed in our experiments. As these puncta fluoresce at a higher intensity than diffuse TDP-43 expression, this may lead to an overall decrease in cytoplasmic/nuclear fluorescence ratio relative to TDP-43_{WT}. Thus, in some cases quantification of nuclear and cytoplasmic puncta may be a useful adjunct to assess the pathogenicity of a given mutation. However, the disease relevance of nuclear inclusions in in vitro studies of TDP-43_{M337V} is unclear: although both intranuclear and cytoplasmic inclusions were reported in a transgenic TDP-43_{M337V} mouse model[43] and it is reminiscent of intranuclear inclusions observed in post-mortem tissue from sporadic FTD patients[9], such inclusions are rare in human disease. In the only neuropathological report to our knowledge that concerns a patient with a *TARDBP* M337V mutation, no mention was made of intranuclear inclusions[44]. We also note that mislocalisation of TDP-43 is not the only mechanism by which *TARDBP* mutations lead to disease: for example, changes in protein stability or interaction partners have also been described[31]. However, we envisage that the mislocalisation assay as implemented here would be a useful tool in a battery of assays to screen novel *TARDBP* variants.

Lastly, we were able to recapitulate the effect of WT CYLD, the FTD-ALS-causative mutation p.M719V and the catalytically inactive mutation p.D681G on subcellular localisation of endogenous TDP-43, which we previously observed in mouse cortical neurons[4]. In comparison to the other experiments used to validate this quantification method, the degree of change in the endogenous TDP-43 cytoplasmic/nuclear ratio between the empty vector, the $CYLD_{WT}$ and the CYLD mutations was very small: e.g., absolute increase in ratio of ~ 0.03–0.04 between $CYLD_{WT}$ and $CYLD_{M719V}$ (Fig. 4s and Fig. S4s). Our ability to detect significant differences for such a subtle change demonstrates the sensitivity of this technique for detecting changes in TDP-43 and FUS localisation in vitro. We note that this assay relies on overexpression of the secondary gene and it would therefore be judicious to perform follow-up studies to examine whether the effect is still observed when the gene is expressed at physiological levels (e.g. by CRISPR/Cas9-editing to introduce candidate gene mutations) and/or in more biologically relevant cells (e.g. induced pluripotent stem cell-derived neurons). However, the utilisation of our quantification method in this format demonstrates what we believe to be its primary use, prioritising potentially pathogenic newly identified FTD- or ALS-associated variants in genes other than *FUS* and *TARDBP* for more in-depth investigation.

An important parameter to consider when visualising mislocalisation of TDP-43 and FUS in exogenous expression assays is the positioning of the fluorescent tag in the TDP-43 or FUS fusion proteins. In this study we utilised a N-terminal GFP tag for FUS constructs, due to the location of its nuclear localisation signal (NLS) at the C-terminus (aa497-526)[45]. Conversely, we used a C-terminal GFP tag for TDP-43, as its NLS is located near the N-terminus of the protein (aa82-98)[46], and TDP-43 forms homodimers via its N-terminus[47,48]. By tagging the protein at the opposite end to its NLS or dimer-binding region we hoped to minimise any effect on the normal localisation pattern of TDP-43 and FUS. Additionally, aggregates of TDP-43 contain C-terminal fragments[49], which may have been undetectable had we used a N-terminal GFP tag. We note that the cytoplasmic/nuclear ratio of exogenous GFP-FUS_{WT} (0.10 ± 0.00; Fig. 1l) was almost identical to that of endogenous FUS in vehicle-treated cells (0.09 ± 0.00; Fig. 2g), implying that this tag does not affect FUS localisation. For TDP-43, the cytoplasmic/nuclear ratio of the GFP-tagged protein (0.75 ± 0.01; Fig. 3k) was much higher than that of endogenous TDP-43 (0.079 ± 0.001; Fig. 4s). This is seen for exogenous expression of TDP-43 even with small peptide tags[19,23]. Nevertheless, we acknowledge that the presence of the larger GFP tag may further affect TDP-43 localisation and represents a limitation of this assay.

A parameter of equivalent importance for detection of endogenous FUS and TDP-43 mislocalisation is selection of an appropriate detection antibody. This is particularly important for TDP-43, where C-terminal TDP-43 fragments observed in FTD and ALS patients[9] contribute to its mislocalisation and aggregation[49]. Antibodies raised against the extreme N-terminus of TDP-43 would therefore not be suitable for a mislocalisation assay, as they would not detect these cleavage products. In contrast, the anti-TDP-43 antibody we used (Proteintech; #10782-2-AP) recognises all major truncated TDP-43 forms[9].

In summary, this study demonstrates a simple methodology for unbiased quantification of TDP-43 and FUS cytoplasmic mislocalisation in vitro. This technique can easily be added to studies utilising qualitative data to strengthen clearly noticeable phenotypes in an unbiased manner, as well as to highlight subtle changes that may have not been previously identified. Utilisation of this fast and cost-effective technique to aid in assessing pathogenicity of gene variants observed in patients with FTD or ALS will help to prioritise these variants for more intensive research efforts into how they cause disease.

Methods

DNA constructs. *CYLD, TARDBP* and *FUS* mutations were introduced into the pCMV6-CYLD, pCMV6-TARDBP and pCMV6-FUS constructs (Origene) by site-directed mutagenesis using the QuikChange Lightning Site-Directed Mutagenesis Kit (Agilent). Mutated *CYLD* and *TARDBP* cDNA sequences were then subcloned, using AsiSI and MluI restriction sites, into the pCMV6-AC-GFP vector (Origene) for expression of C-terminal GFP-tagged CYLD and TDP-43 proteins, respectively. Mutated *FUS* cDNA sequences were subcloned similarly into the pCMV6-AN-GFP vector (Origene) for expression of N-terminal GFP-tagged FUS protein, to avoid interference of the GFP tag with the C-terminal NLS of the FUS protein[45]. All clones were verified by restriction digestion and sequence analysis.

Cell culture. HEK293 and SH-SY5Y were purchased from ATCC and authenticated by STR analysis prior to use in this study. HEK293 cells were maintained in Eagle's Minimum Essential Medium (EMEM; Gibco) and SH-SY5Y cells in Dulbecco's Modified Eagle's Medium/Nutrient Mixture F-12 (DMEM/F12; 1:1 mixture; Gibco) each containing 10% heat-inactivated fetal calf serum (Sigma-Aldrich). For immunocytochemistry, 8-well chamber slides (Ibidi) were coated with 0.005% poly-L-lysine (Sigma-Aldrich) for 1 h and then washed twice with Dulbecco's phosphate-buffered saline (DPBS; Gibco). SH-SY5Y cells were seeded at $5–7.5 \times 10^4$ cells/well and HEK293 cells were seeded at 8×10^4 cells/well. After 24 h, cells were transfected with GFP constructs (250 ng/well) for 24 (HEK293) or 48 (SH-SY5Y) hours using Lipofectamine 3000 (0.75 µL/well; Invitrogen) as per the manufacturer's protocol. For the staurosporine experiment, cells were incubated for 48 h after seeding, then treated for 5 h with 0.1, 1 or 10 µM staurosporine, to induce apoptosis. Staurosporine dilutions were prepared from a 1 mM staurosporine stock solution dissolved in dimethyl sulfoxide (DMSO; Sigma-Aldrich). All vehicle and staurosporine treatment groups were adjusted to a final concentration of 1% DMSO.

Immunocytochemistry. Transfected or drug-treated cells were fixed in 4% paraformaldehyde (PFA) in PBS for 20 min in the dark. For visualisation of exogenous TDP-43 and FUS, cells were then washed twice with DPBS and mounted using DAKO fluorescent mounting medium containing 4′,6-diamidino-2-phenylindole (DAPI; Agilent). For visualisation of endogenous TDP-43 and FUS, non-specific background staining was blocked after cell fixation using 1% bovine serum albumin (BSA) in PBS for 30 min. Cells were then incubated overnight at 4 °C with rabbit anti-TDP-43 (1:500; Proteintech #10782-2-AP) or rabbit anti-FUS (1:500, Proteintech #11570-1-AP) antibodies. The next day, cells underwent 2 × 5-min washes with DPBS, incubation with rabbit Alexa Fluor-647 secondary antibody (1:500; Invitrogen #A-21244) for 1 h, followed by 2 × 5-min washes and mounting as above. Cells were imaged for fluorescence intensity quantification with a 40 × objective on a Nikon A1R confocal microscope. Images of representative cells were obtained with a 100 × objective for figure preparation. Laser intensity, gain and offset settings were kept constant and at least five random fields of view were imaged for each experimental replicate.

Fluorescence intensity quantification. Quantification of changes in the cellular localisation of TDP-43 or FUS between the nucleus and the cytoplasm was done by utilising CellProfiler 3.1.9 software (Broad Institute, Cambridge, MA)[28]. To prepare images for analysis, ND2 microscope files were converted to TIFFs, blinded and split into individual wavelength channel images using ImageJ (National Institutes of Health, Bethesda MD)[36]. In CellProfiler, the DAPI channel was analysed first using the *Identify Primary Objects* module and a global, three-class Otsu thresholding method. This allowed for identification and separation of each nucleus within an image. Strict filtering for cell diameter (30–60 pixels) eliminated any irregular or overlapped nuclei that were present. TDP-43- or FUS-positive cells were also identified using the *Identify Primary Objects* module. Cell diameter filtering for this step had a much larger range and was dependent on experimental conditions and cell type (20–150 pixels). The *Relate* and *Filter* modules were used to link filtered nuclei to TDP-43- or FUS-positive cells. Centroid distance filtering, which limits the distance between the centre of the nucleus and the centre of the cytoplasm (maximum 40 pixels) was also applied to remove any debris or abnormal cells that may be fluorescing in the TDP-43/FUS channel. For the experiments quantifying endogenous TDP-43 in cells expressing GFP-tagged CYLD constructs, additional steps in the analysis were required. GFP-positive CYLD cells were identified in the same way as TDP-43- or FUS-positive cells using the *Identify Primary Objects* module, described above. However, prior to this, TDP-43-positive cells were identified by association with their corresponding nuclei, using the *Identify Secondary Objects* module. The watershed-image method was used with global, three-class Otsu thresholding. Size filtering was also applied (maximum 3000 pixels) to remove any clumped cells. The *Relate* and *Filter* modules were used to select only TDP-43-positive cells that were also positive for GFP. TDP-43- and GFP-positive cells were then linked to their corresponding nuclei using the *Relate* and *Filter* modules described above. For all experiments, in each TDP-43/FUS-positive cell, the nucleus and cytoplasm were separated into individual objects using the *Identify Tertiary Objects* module. Integrated (total) fluorescence intensity for both cellular compartments were then measured from the TDP-43/FUS channel image using the *Measure Object Intensity* module. Using these measurements, the cytoplasmic to nuclear ratio of TDP-43 or FUS was calculated for 300 cells per group, for each of the six replicates of the experiment. All filtering and thresholding steps in each experimental pipeline were kept consistent throughout all experimental replicates. Filtering values were specific to each experiment and require adjustment for different cell types and microscope parameters.

Statistical analysis. Data are presented as mean ± standard error of the mean (SEM) from at least six independent experiments of n = 300 cells. Mean fluorescent intensity of TDP-43 or FUS across six biological replicates was in most cases compared by repeated measures one-way ANOVA and Dunnett's multiple comparisons test. The effect of CYLD on endogenous TDP-43 was analysed using repeated measures one-way ANOVA and Sidak's multiple comparisons test. All statistical analyses were performed using GraphPad Prism 9. Significance for all tests was set at $p < 0.05$.

Data availability

The datasets and materials generated during the current study are available from the corresponding author on reasonable request.

Received: 6 April 2021; Accepted: 6 July 2021
Published online: 21 July 2021

References

1. Lillo, P. & Hodges, J. R. Frontotemporal dementia and motor neurone disease: Overlapping clinic-pathological disorders. *J. Clin. Neurosci.* **16**, 1131–1135 (2009).
2. Burrell, J. R. *et al.* The frontotemporal dementia-motor neuron disease continuum. *Lancet* **388**, 919–931 (2016).
3. Abramzon, Y. A., Fratta, P., Traynor, B. J. & Chia, R. The overlapping genetics of amyotrophic lateral sclerosis and frontotemporal dementia. *Front. Neurosci.* **14**, 1–10 (2020).
4. Dobson-Stone, C. *et al.* CYLD is a causative gene for frontotemporal dementia-amyotrophic lateral sclerosis. *Brain* **143**, 783–799 (2020).
5. Prasad, A., Bharathi, V., Sivalingam, V., Girdhar, A. & Patel, B. K. Molecular mechanisms of TDP-43 misfolding and pathology in amyotrophic lateral sclerosis. *Front. Mol. Neurosci.* **12**, 1–36 (2019).
6. Mackenzie, I. R. A., Rademakers, R. & Neumann, M. TDP-43 and FUS in amyotrophic lateral sclerosis and frontotemporal dementia. *Lancet Neurol.* **9**, 995–1007 (2010).
7. Vance, C. *et al.* Mutations in FUS, an RNA processing protein, cause familial amyotrophic lateral sclerosis type 6. *Science* **323**, 1208–1211 (2009).
8. Mackenzie, I. R. A. *et al.* Distinct pathological subtypes of FTLD-FUS. *Acta Neuropathol.* **121**, 207–218 (2011).
9. Neumann, M. *et al.* Ubiquitinated TDP-43 in frontotemporal lobar degeneration and amyotrophic lateral sclerosis. *Science* **314**, 130–133 (2006).
10. Cairns, N. J. *et al.* Neuropathologic diagnostic and nosologic criteria for frontotemporal lobar degeneration: Consensus of the consortium for frontotemporal lobar degeneration. *Acta Neuropathol.* **114**, 5–22 (2007).
11. Sreedharan, J. *et al.* TDP-43 Mutations in familial and sporadic amyotrophic lateral sclerosis. *Science* **319**, 1668–1672 (2008).
12. Kwiatkowski, T. J. *et al.* Mutations in the FUS/TLS gene on chromosome 16 cause familial amyotrophic lateral sclerosis. *Science* **323**, 1205–1208 (2009).
13. Lagier-tourenne, C., Polymenidou, M. & Cleveland, D. W. TDP-43 and FUS/TLS: Emerging roles in RNA processing and neurodegeneration. *Hum. Mol. Genet.* **19**, 46–64 (2010).
14. Brown, R. H. & Al-Chalabi, A. Amyotrophic lateral sclerosis. *N. Engl. J. Med.* **377**, 162–172 (2017).
15. Younes, K. & Miller, B. L. Frontotemporal dementia: Neuropathology, genetics, neuroimaging, and treatments. *Psychiatr. Clin. North Am.* **43**, 331–344 (2020).
16. Deng, Q. *et al.* FUS is phosphorylated by DNA-PK and accumulates in the cytoplasm after DNA damage. *J. Neurosci.* **34**, 7802–7813 (2014).
17. Naumann, M. *et al.* Impaired DNA damage response signaling by FUS-NLS mutations leads to neurodegeneration and FUS aggregate formation. *Nat. Commun.* **9**, 335 (2018).
18. Walker, A. K. *et al.* ALS-associated TDP-43 induces endoplasmic reticulum stress, which drives cytoplasmic TDP-43 accumulation and stress granule formation. *PLoS One* **8**, 1–12 (2013).
19. Han, J. H. *et al.* ALS/FTLD-linked TDP-43 regulates neurite morphology and cell survival in differentiated neurons. *Exp. Cell Res.* **319**, 1998–2005 (2013).
20. Kabashi, E. *et al.* Gain and loss of function of ALS-related mutations of TARDBP (TDP-43) cause motor deficits in vivo. *Hum. Mol. Genet.* **19**, 671–683 (2009).
21. Wobst, H. J. *et al.* Cytoplasmic relocalization of TAR DNA-Binding Protein 43 is not sufficient to reproduce cellular pathologies associated with ALS in vitro. *Front. Mol. Neurosci.* **10**, 1–13 (2017).
22. Arnold, E. S. *et al.* ALS-linked TDP-43 mutations produce aberrant RNA splicing and adult-onset motor neuron disease without aggregation or loss of nuclear TDP-43. *Proc. Natl. Acad. Sci.* **110**, E736–E745 (2013).
23. Araki, W. *et al.* Disease-associated mutations of TDP-43 promote turnover of the protein through the proteasomal pathway. *Mol. Neurobiol.* **50**, 1049–1058 (2014).
24. Mutihac, R. *et al.* TARDBP pathogenic mutations increase cytoplasmic translocation of TDP-43 and cause reduction of endoplasmic reticulum Ca^{2+} signaling in motor neurons. *Neurobiol. Dis.* **75**, 64–77 (2015).
25. Kim, S. H., Zhan, L., Hanson, K. A. & Tibbetts, R. S. High-content RNAi screening identifies the type 1 inositol triphosphate receptor as a modifier of TDP-43 localization and neurotoxicity. *Hum. Mol. Genet.* **21**, 4845–4856 (2012).
26. Kim, M. *et al.* Modeling of frontotemporal dementia using iPSC technology. *Int. J. Mol. Sci.* **21**, 1–16 (2020).
27. Fujimori, K. *et al.* Modeling sporadic ALS in iPSC-derived motor neurons identifies a potential therapeutic agent. *Nat. Med.* **24**, 1579–1589 (2018).
28. Carpenter, A. E. *et al.* Cell Profiler: Image analysis software for identifying and quantifying cell phenotypes. *Genome Biol.* **7**, R100 (2006).
29. Bosco, D. A. *et al.* Mutant FUS proteins that cause amyotrophic lateral sclerosis incorporate into stress granules. *Hum. Mol. Genet.* **19**, 4160–4175 (2010).
30. Gitcho, M. A. *et al.* TDP-43 A315T mutation in familial motor neuron disease. *Ann. Neurol.* **63**, 535–538 (2008).
31. Buratti, E. Functional significance of TDP-43 mutations in disease. *Adv. Genet.* **91**, 1–53 (2015).
32. Kabashi, E. *et al.* TARDBP mutations in individuals with sporadic and familial amyotrophic lateral sclerosis. *Nat. Genet.* **40**, 572–574 (2008).
33. Rutherford, N. J. *et al.* Novel mutations in TARDBP(TDP-43) in patients with familial amyotrophic lateral sclerosis. *PLoS Genet.* **4**, 1–8 (2008).
34. Bignell, G. R. *et al.* Identification of the familial cylindromatosis tumour-suppressor gene. *Nat. Genet.* **25**, 160–165 (2000).
35. Rajan, N. & Ashworth, A. Inherited cylindromas: Lessons from a rare tumour. *Lancet Oncol.* **16**, e460–e469 (2015).
36. Schneider, C. A., Rasband, W. S. & Eliceiri, K. W. NIH Image to ImageJ: 25 years of image analysis. *Nat. Methods* **9**, 671–675 (2012).
37. Acosta, J. R. *et al.* Mutant human FUS is ubiquitously mislocalized and generates persistent stress granules in primary cultured transgenic zebrafish cells. *PLoS One* **9**, e90572 (2014).
38. Moreno, F. *et al.* A novel mutation P112H in the TARDBP gene associated with frontotemporal lobar degeneration without motor neuron disease and abundant neuritic amyloid plaques. *Acta Neuropathol. Commun.* **3**, 1–13 (2015).
39. Van Deerlin, V. M. *et al.* TARDBP mutations in amyotrophic lateral sclerosis with TDP-43 neuropathology: A genetic and histopathological analysis. *Lancet Neurol.* **7**, 409–416 (2008).
40. Gelpi, E., van der Zee, J., Turon Estrada, A., Van Broeckhoven, C. & Sanchez-Valle, R. TARDBP mutation p.Ile383Val associated with semantic dementia and complex proteinopathy. *Neuropathol. Appl. Neurobiol.* **40**, 225–230 (2014).
41. Pansarasa, O. *et al.* Lymphoblastoid cell lines as a model to understand amyotrophic lateral sclerosis disease mechanisms. *DMM Dis. Model. Mech.* **11**, 1–12 (2018).
42. Gianini, M. *et al.* TDP-43 mutations link amyotrophic lateral sclerosis with R-loop homeostasis and R loop-mediated DNA damage. *PLoS Genet.* **16**, 1–23 (2020).
43. Xu, Y.-F. *et al.* Expression of mutant TDP-43 induces neuronal dysfunction in transgenic mice. *Mol. Neurodegener.* **6**, 73 (2011).
44. Tamaoka, A. *et al.* TDP-43 M337V mutation in familial amyotrophic lateral sclerosis in Japan. *Intern. Med.* **49**, 331–334 (2010).
45. Vance, C. *et al.* ALS mutant FUS disrupts nuclear localization and sequesters wild-type FUS within cytoplasmic stress granules. *Hum. Mol. Genet.* **22**, 2676–2688 (2013).
46. Winton, M. J. *et al.* A90V TDP-43 variant results in the aberrant localization of TDP-43 in vitro. *FEBS Lett.* **582**, 2252–2256 (2008).

47. Zhang, Y. J. *et al.* The dual functions of the extreme N-terminus of TDP-43 in regulating its biological activity and inclusion formation. *Hum. Mol. Genet.* **22**, 3112–3122 (2013).
48. Sasaguri, H. *et al.* The extreme N-terminus of TDP-43 mediates the cytoplasmic aggregation of TDP-43 and associated toxicity in vivo. *Brain Res.* **1647**, 57–64 (2016).
49. Igaz, L. M. *et al.* Expression of TDP-43 C-terminal fragments in vitro recapitulates pathological features of TDP-43 proteinopathies. *J. Biol. Chem.* **284**, 8516–8524 (2009).

Acknowledgements

The authors acknowledge the facilities and technical assistance of Microscopy Australia at the Australian Centre for Microscopy and Microanalysis at the University of Sydney. This research was funded by the National Health and Medical Research Council of Australia (NHMRC) Project Grant 1140708 (to C.D.-S. and J.B.K.), by NHMRC Boosting Dementia Research Leadership Fellowship 1138223 (to C.D.-S.) and the University of Sydney. J.B.K. is supported by NHMRC Project Grant 1163249, NHMRC-JPND Grant 1151854 and NHMRC Dementia Research Team Grant 1095127.

Author contributions

L.J.O., J.B.K. and C.D.-S. conceived the study. S.U., L.F., M.H. and L.M.B. generated and sequence-verified mutant cDNA constructs. L.J.O. carried out TDP-43 and FUS localisation experiments. L.J.O. and C.D.-S. participated in data analysis. L.J.O. and C.D.-S. drafted the manuscript. All authors read and approved the final manuscript.

Competing interests

The authors declare no competing interests.

Additional information

Supplementary Information The online version contains supplementary material available at https://doi.org/10.1038/s41598-021-94225-1.

Correspondence and requests for materials should be addressed to C.D.-S.

Reprints and permissions information is available at www.nature.com/reprints.

Publisher's note Springer Nature remains neutral with regard to jurisdictional claims in published maps and institutional affiliations.